Quantum Coherence Engineering in the Integer Quantum Hall Regime

P-A. Huynh,[1] F. Portier,[1] H. le Sueur,[2] G. Faini,[2] U. Gennser,[2] D. Mailly,[2] F. Pierre,[2] W. Wegscheider,[3] and P. Roche[1,*]

[1]*CEA, SPEC, Nanoelectronics Group, URA 2464, F-91191 Gif-sur-Yvette, France*
[2]*CNRS, LPN, Phynano Team, route de Nozay, 91460 Marcoussis, France*
[3]*Laboratory for Solid State Physics, ETH Zürich, CH-8093 Zürich, Switzerland*

(Received 16 February 2012; published 18 June 2012)

We present an experiment where the quantum coherence in the edge states of the integer quantum Hall regime is tuned with a decoupling gate. The coherence length is determined by measuring the visibility of quantum interferences in a Mach-Zehnder interferometer as a function of temperature, in the quantum Hall regime at a filling factor 2. The temperature dependence of the coherence length can be varied by a factor of 2. The strengthening of the phase coherence at finite temperature is shown to arise from a reduction of the coupling between copropagating edge states. This opens the way for a strong improvement of the phase coherence of quantum Hall systems. The decoupling gate also allows us to investigate how interedge state coupling influences the quantum interferences' dependence on the injection bias. We find that the finite bias visibility can be decomposed into two contributions: a Gaussian envelope which is surprisingly insensitive to the coupling, and a beating component which, on the contrary, is strongly affected by the coupling.

DOI: 10.1103/PhysRevLett.108.256802 PACS numbers: 73.43.Fj, 03.65.Yz, 73.23.Ad

Rare are the cases where quantum coherence can simply be controlled with a knob. This is because phase coherence is generally limited by the coupling of the system to its environment, and this coupling is not easily controlled. In a two-dimensional electron gas in the integer quantum Hall (IQH) regime such a control is possible, due to the simplicity of the environment. In this regime, electrical transport occurs through one-dimensional chiral channels localized on the edges of the electron gas. Chirality reduces electron scattering, increasing the electron coherence length [1]. This has motivated recent theoretical proposals to use these edge states for quantum information experiments, and has renewed interest in the community for precise investigations of quantum coherence and energy relaxation in the IQH regime. When two edge states are present, they constitute their own mutual environment. More specifically, the thermal charge noise in the one limits the phase coherence in the other [2,3]. Taking advantage of this, we have designed a new Mach-Zehnder interferometer (MZI) where we measure quantum interferences in the outer edge state while controlling the trajectory of the inner one with additional gates. This allows us to tune the coupling between edge states, resulting in an unprecedented way to control the coherence in the IQH regime. Our measurements show that one can increase the coherence length by nearly a factor of 2.

The integer quantum Hall regime is obtained by applying a high magnetic field perpendicular to a two-dimensional gas at low temperature. When the number of electrons per quantum of flux (the filling factor) is an integer, the electrical transport occurs through one-dimensional chiral modes on the edge of the sample: the edge states. The number of these edge states is equal to the filling factor. This one-dimensional chiral transport has made new quantum experiments with electrons possible. For example, quantum interference experiments in the IQH regime have allowed the first observation of two electron interferences [4], a first step toward the observation of the violations of Bell's inequalities [5]. Alternatively, combining a single electron gun [6] with a Mach-Zehnder interferometer [7,8] could permit the realization of Wheeler's delayed choice gedanken experiment [9] with electrons. However, these electronic versions of optical experiments suffer from one major problem: an electron carries a charge with which it interacts with the surrounding world, leading to a finite quantum coherence length and a finite energy exchange length. Recently, both lengths have been measured in the IQH regime at a filling factor 2, definitively showing the role of the interaction between the inner and outer edge state [2,3,10].

While the dependence of the coherence length with temperature has been clearly identified to result from the thermal charge noise in the neighboring edge state [3], it has not yet been possible to clearly identify the role of energy exchanges on the repeatedly observed but poorly understood Gaussian shape of the visibility as a function of the bias voltage [11–13]. It has been demonstrated recently that the energy exchange between the edge states, which form at a filling factor 2, can be frozen by opening a gap in the excitations of the inner edge state (IES). This is done by forcing the IES on a small closed loop trajectory of length L_δ of the order of 8 μm, leading to an energy spacing $E_\delta \sim h v_D / L_\delta \sim 50$ μeV, and hence freezing energy exchange below this value [14]. Inspired by theses findings, we have designed a new MZI with additional gates $DG1$ and $DG2$ used to localize the IES on loops typically 8 μm

long (see Fig. 1). The goal of these new gates is twofold: first, to freeze the charge fluctuations in the nearby environment and hence increase the finite temperature coherence length l_φ, and second, to check if finite bias energy exchanges are involved in the finite bias visibility decrease. One would expect in this case an enhancement of the robustness of quantum interference with the bias. While we do clearly observe an enhancement of the finite temperature coherence length that we prove to be due to a reduction of the coupling to the environment, the robustness of the visibility with the bias voltage is surprisingly poorly affected by the decoupling gates.

The MZI is realized with a high mobility two-dimensional electron gas with a density of 1.1×10^{11} cm^{-2} and a mobility of 3×10^6 cm^2 V^{-1} s^{-1}. The measurements have been performed at a filling factor 2 with a 2.63 T magnetic field. The two beam splitters of the MZI are quantum point contacts $G1$ and $G2$ with transmission probability of the outer edge state (OES) $\mathcal{T}_1$ and $\mathcal{T}_2$ (the IES is fully reflected). Each arm of the MZI is 11.8 μm long. The differential transmission $\mathcal{T} = dI_T/dI_0$, I_T being the transmitted current and I_0 the incoming current, is measured with standard lock-in techniques with a 2 μV_{RMS} excitation. Thanks to the additional gate G_0, the IES and OES can be fed with different biases V_1 and V_2, respectively. The interference pattern is revealed by ramping the voltage on the side gate G_C, which changes the Aharonov-Bohm flux ϕ through the area defined by the two arms of the interferometer $\mathcal{T} = \mathcal{T}_{\mathrm{mean}}[1 + \mathcal{V}\sin(\varphi)]$, $\mathcal{V}$ being the visibility proportional to $\exp(-T/T_\varphi)\sqrt{\mathcal{T}_1\mathcal{R}_2\mathcal{T}_2\mathcal{R}_1}/(\mathcal{T}_1\mathcal{T}_2 + \mathcal{R}_1\mathcal{R}_2)$. T is the temperature, $\mathcal{R}_i = 1 - \mathcal{T}_i$, and $\varphi = 2\pi\phi/\phi_0$ where ϕ is the magnetic flux through the area defined by the two arms of the MZI. Both gates DG_i fully transmit the IES at 0.3 V and fully reflect it at 0.1 V.

Figure 2 shows the visibility $\mathcal{V}$ of quantum interferences at the base temperature of 25 mK, the transmission probability through the upper arm, and the transmission through the MZI averaged over 10 Aharonov-Bohm periods. One can see that DG_1 has a great impact on the visibility, which is enhanced by a factor of the order of 2 between full transmission and full reflection of the OES. Acting on DG_2 also increases the visibility, but much less. The visibility saturates when the IES is fully reflected, before decreasing at lower V_{DG_1}. This decrease is most probably due to the deformation of the OES leading to an imbalance in the two arms trajectory length and/or the detuning of the MZI, which is illustrated by the departure of the mean transmission from the 0.25 value (squares on Fig. 2). The decrease is accompanied by large drops in the visibility, associated with sudden phase shifts in the interference pattern when sweeping the voltage of the side gate GC (not shown). We attribute these to variations in the charge in the islands formed by the inner edge states.

We wish to stress that the effect of DG_1 is not a reduction of the thermal smearing which could occur in case of an imbalance of the time of flight through the two arms. Thermal smearing leads to a visibility dependence $\mathcal{V} \propto T\sinh^{-1}(T/T_T) \sim \exp(-T/T_T)$ for $T \gg T_T$ with

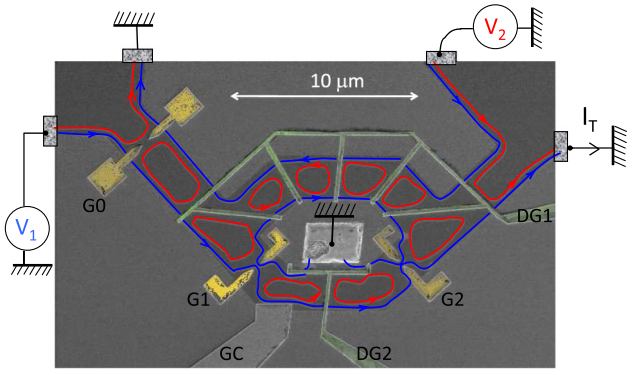

FIG. 1 (color online). Scanning electronic microscope view of the sample: the quantum point contacts $G1$ and $G2$ are the beam splitters of the MZI. Additional gates $DG1$ and $DG2$ are placed on the upper and lower arms to force the inner edge state into small closed loops. The interferences are realized on the outer edge state. The two edge states are fed with different bias voltage with the aid of $G0$: $V1$ for the outer one, and $V2$ for the inner one. The variation of the phase with respect to $V2$ allows us to determine the coupling between the two edge states. The picture was taken before the final fabrication step, where bridges are realized to connect both sides of the quantum point contacts and the small Ohmic contact in the center of the figure.

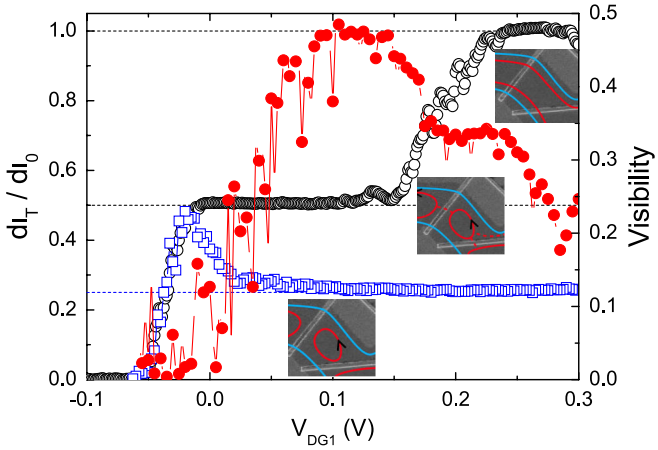

FIG. 2 (color online). Solid (red) dot: Visibility of quantum interferences for different values of V_{DG_1} as a function of the bias voltage at 25 mK. Open (black) dot: Transmission probability through the upper arm of the interferometer. Open (blue) square: Mean transmission through the MZI when revealing interference, the IES being fully reflected by $G0$. The departure from the 0.25 value below $V_{DG_1} \sim 0.1$ V indicates a detuning of the MZI due to DG_1. The trajectories of both edge states are shown schematically for different values of V_{DG_1} in the inserted scanning electronic microscope pictures.

$T_T^{-1} = \pi k_B/e \times \partial\varphi/\partial V_{DS}$, where $\partial\varphi/\partial V_{DS}$ is the phase dependance of the Aharonov-Bohm oscillations as a function of the dc bias applied on the MZI [3,15]. T_T^{-1} determined from the variation of the AB phase with the bias is represented in Fig. 3. T_T^{-1}, which is of the order of 20 K^{-1}, has a negligible impact on the visibility $\mathcal{V}$. Figure 3 illustrates the underlying physics leading to the coherence enhancement. It proves that the coherence is modified because DG_1 allows us to change the coupling of the OES with its environment. Figure 3 is constructed in the following way. We first measure the temperature dependence of $\mathcal{V}$ for different values of V_{DG_1}. It shows an exponential behavior $\mathcal{V} \propto \exp(-T/T_\varphi)$, with the decoherence T_φ^{-1} decreasing when decreasing V_{DG_1}. The interedge state coupling, $V_0^{-1} = (2\pi^{-1})\partial\varphi/\partial V_2$ is simultaneously measured, using the method of Ref. [3]: one feeds the IES with a potential V_2 while the OES remains at equilibrium. The IES plays the role of a side gate used to reveal interferences in the OES.

The variations of T_φ^{-1} and V_0^{-1} with V_{DG_1} are remarkably similar, strongly suggesting that these two quantities have a common microscopic origin. Assuming that the dephasing is a sum of the dephasings in the upper and the lower arms, $T_\varphi^{-1} = T_{\varphi,\mathrm{up}}^{-1} + T_{\varphi,lo}^{-1}$, with $T_{\varphi,\mathrm{up}}^{-1} = \alpha V_0^{-1}$ following

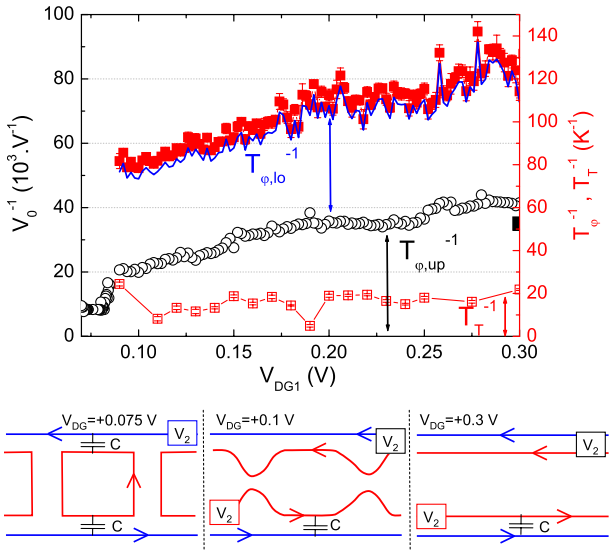

FIG. 3 (color online). Open circles: Coupling V_0^{-1} between the IES and the OES (left axis). Filled squares (right axis): Measured dephasing $T_\varphi^{-1} = -\partial \ln(\mathcal{V})/\partial T$. Solid line (right axis): Measured T_φ^{-1} after subtracting the thermal averaging (see Supplemental Material [20]). Open squares (right axis): T_T^{-1}, calculated from the phase variation of the bias (see text). The solid black square at $V_{DG1} = 0.3$ V represents the dephasing $T_{\varphi,\mathrm{up}}^{-1}$ in the upper arm, deduced from a which-path experiment. The scale of the left axis has been adjusted so that the dephasing $T_{\varphi,\mathrm{up}}^{-1}$ of the upper arm corresponding to V_0^{-1} can be read on the right axis. The lower panel is a sketch of the edge state coupling for different values of V_{DG1}.

Ref. [3], one can set the proportionality factor α so that the variations of V_0^{-1} reproduce those of T_φ^{-1}. The scales of Fig. 3 are adjusted following this procedure, such that the open black circles represent V_0^{-1} to the left and the corresponding $T_{\varphi,\mathrm{up}}^{-1}$ to the right. Independently, we deduced $T_{\varphi,\mathrm{up}}^{-1}$ from a "which-path" experiment, where the AB interferences of the outer edge state were washed out by shot noise produced in the inner edge state. This was done for $V_{DG1} = 0.3$ V by setting the transmission of the IES on $G0$ at one half and applying various bias voltages on V_2. Following Ref. [3], we can extract $T_{\varphi,\mathrm{up}}^{-1}$ from the observed variations of the visibility with V_2. The obtained value, 51 ± 2 K^{-1}, represented by the solid black square in Fig. 3, is in remarkable agreement with the estimation based on the variations of V_0^{-1}. Note that this experiment is *not* possible for lower values of V_{DG_1}, when the decoupling gate DG depletes the 2DEG, as this introduces partial reflections of the inner edge state. As expected, the difference between T_φ^{-1} and the adjusted $T_{\varphi,\mathrm{up}}^{-1}$, corresponding to the dephasing in the lower arm, is almost independent of $DG1$.

We now focus on the behavior at full reflection of the IES (around $V_{DG1} = 0.08$ V). The coupling V_0^{-1} changes abruptly by a factor of the order of 2. As sketched in the lower panel of Fig. 3, the decrease of the coupling is not due to a variation of the actual coupling between the two edge states. In fact, here the IES is no longer at the potential V_2. The measured variation of the AB phase with V_2 results from the coupling with the counterpropagating OES at potential V_2 through the small loop formed by the IES. This process leads to a factor 2 in the coupling, corresponding to two geometrical capacitances in series, each mimicking the local coupling between the two neighboring edge states.

Unexpectedly, the base temperature visibility reaches a maximum (around $V_{DG1} = 0.1$ V) before decreasing (see Fig. 2), indicating that the variations of V_0 no longer imply a variation of T_φ [16]. Following the approach of Refs. [3,17], only charge fluctuations on a time scale longer than the time of flight through the MZI account for the dephasing. Here the static charge in the small loops should be frozen and electron-hole excitations are expected to occur only at temperatures larger than E_δ/k_B, eliminating low temperature charge fluctuations on the small loops. Hence T_φ^{-1} should result from thermal charge noise in the counterpropagating OES coupled to the interfering OES through the loops: T_φ^{-1} should be proportional to V_0^{-1}, even when the loops are formed. The contradiction between this simple model and our observations may result from different causes. For example, the freezing of charge fluctuations could be compensated by an imbalance of electron trajectories in both arms leading to thermal averaging; or the drift velocity may be overestimated, leading to an overestimation of the energy gap of the loops. Also, it could be that the charge noise due to the dissipative part of the

coupling between the interfering edge state and the metallic gates leads to decoherence [17], or that another mechanism implying coupling between edge states [18] is responsible for decoherence. For the time being, we lack experimental data to answer to these questions.

Another aspect that we address in this experiment is the role of interedge state coupling and energy exchange [10] on the finite bias visibility. Although several theoretical works have attempted to explain the unexpected multiple lobe structure observed in the variations of the visibility with bias voltage [11,12,19], so far no scenario has been fully validated experimentally. In particular, the Gaussian envelop of the visibility $\mathcal{V} \propto \exp(-V^2/2V_l^2)$ revealed in Ref. [11] and also observed in Fabry-Pérot interferometers [13] has not been accounted for. In Fig. 4, the visibility as a function of the bias is plotted for different values of V_{DG1}. As already observed [12,19], a side lobe structure shows up, with a first lobe around $V_1 = 20\ \mu$V, and a much smaller one around $V_1 \simeq 40\ \mu$V. When the zero bias visibility is enhanced by decreasing V_{DG1}, the width of the central lobe $\sim V_l$ is hardly affected, even when the IES is fully reflected ($V_{DG1} \sim 0.08$ V). This result points towards the fact that if indeed [14] energy exchanges are frozen, they are not the main process leading to the finite bias visibility decrease. It also shows that the interedge coupling is not involved in the mechanism leading to the Gaussian envelope.

Additional information derived from this measurement is the evolution of the second minimum of the visibility (see Supplemental Material [20]). In the present experiment, as we are able to control the coupling between the edge states, we can make a comparison between our measurements and the theory of Levkivskyi and Sukhorukov [18] where the coupling between edge states is the basic ingredient to explain the presence of the multiple side lobe structure. In this theory, a charge excitation in one edge state is decomposed into two coupled modes, a neutral one (with speed v) and a charged one (with speed u) delocalized on the two edge states. One expects $u \gg v$. There is a simple relation between our coupling parameter V_0 and v: $eV_0 = \pi\hbar v/L$, assuming the upper and lower arms of the interferometer have equal lengths L. Beating between the two modes leads to a visibility of quantum interferences $\propto |\cos[eV_1L/(2\hbar v)]| = |\cos(V_1/V_C)|$ with $V_C = 2\hbar v/(eL) = V_0/(2\pi)$. The finite bias visibility that we measure is very well fitted by a combination of a Gaussian envelope times a cosine term (see Ref. [12] and the Supplemental Material [20]). The first minimum is mainly determined by V_l, poorly affected by the coupling between edge sates (see Fig. 5). The second minimum is mainly determined by the cosine term. In Fig. 5 one can notice that the measured period of the finite bias visibility, V_C, is proportional to the measured coupling V_0, with a proportionality factor of the same order of magnitude as the predictions of Ref. [18]. It is however difficult to make a quantitative comparison as we control the coupling in only one arm of the MZI. Nonetheless, these results definitively show that the underlying mechanism leading to the higher order minima of the side lobe structure involves the interaction between the two edge states.

To summarize, we have strongly enhanced the quantum coherence in the integer quantum Hall regime at a filling factor 2 by protecting the interfering edge state from the thermal charge noise of its environment. Two components of the finite bias visibility have been identified: a Gaussian

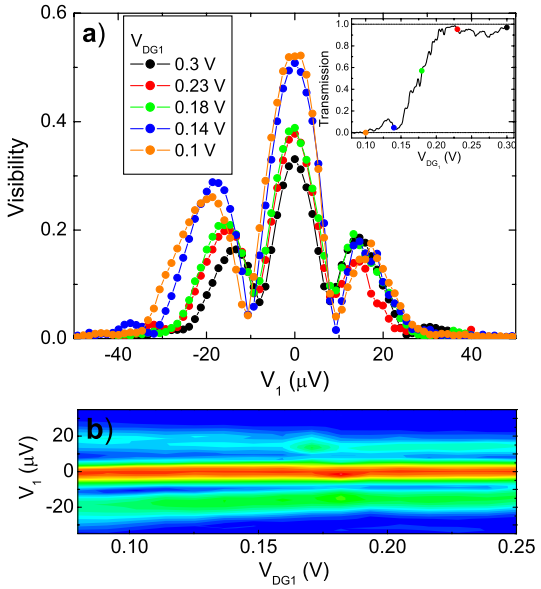

FIG. 4 (color online). (a) Visibility as a function of the bias voltage for different polarizations of $DG1$. Inset: Transmission of the IES through the upper arm of the MZI as a function of V_{DG1}. (b) Two-dimensional color plot of the visibility normalized to the zero bias visibility as a function of V_{DG1} and V_1.

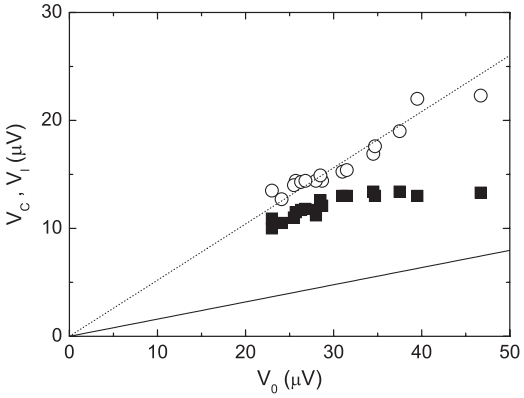

FIG. 5. V_C (open dots) and V_l (black squares) as a function of the coupling between the two edge states characterized by V_0. The dashed line is a guide for the eye. The solid line is the theoretical prediction [18] assuming the same interedge state coupling in both arms of the interferometer.

envelope, poorly affected by the interedge state coupling and, a beating term strongly dependent on the coupling between edge states as recently proposed by a theory.

P. R. thanks E. Sukhorukov for stimulating discussions. This work has been supported by the ANR Grant No. IQHAR (ANR-2011-BS04-022-01).

*patrice.roche@cea.fr

[1] T. Martin and S. Feng, Phys. Rev. Lett. **64**, 1971 (1990).
[2] P. Roulleau, F. Portier, P. Roche, A. Cavanna, G. Faini, U. Gennser, and D. Mailly, Phys. Rev. Lett. **100**, 126802 (2008).
[3] P. Roulleau, F. Portier, P. Roche, A. Cavanna, G. Faini, U. Gennser, and D. Mailly, Phys. Rev. Lett. **101**, 186803 (2008).
[4] I. Neder, N. Ofek, Y. Chung, M. Heiblum, D. Mahalu, and V. Umansky, Nature (London) **448**, 333 (2007).
[5] P. Samuelsson, E. V. Sukhorukov, and M. Büttiker, Phys. Rev. Lett. **92**, 026805 (2004).
[6] G. Féve, A. Mahé, J.-M. Berroir, T. Kontos, B. Plaçais, D. C. Glattli, A. Cavanna, B. Etienne, and Y. Jin, Science **316**, 1169 (2007).
[7] Y. Ji, Y. Chung, D. Sprinzak, M. Heiblum, D. Mahalu, and H. Shtrikman, Nature (London) **422**, 415 (2003).
[8] G. Haack, M. Moskalets, J. Splettstoesser, and M. Büttiker, Phys. Rev. B **84**, 081303(R) (2011).
[9] V. Jacques, E. Wu, F. Grosshans, F. Treussart, P. Grangier, A. Aspect, and J.-F. Roch, Science **315**, 966 (2007).
[10] H. le Sueur, C. Altimiras, U. Gennser, A. Cavanna, D. Mailly, and F. Pierre, Phys. Rev. Lett. **105**, 056803 (2010).
[11] P. Roulleau, F. Portier, D. C. Glattli, P. Roche, A. Cavanna, G. Faini, U. Gennser, and D. Mailly, Phys. Rev. B **76**, 161309(R) (2007).
[12] L. V. Litvin, A. Helzel, H. P. Tranitz, W. Wegscheider, and C. Strunk, Phys. Rev. B **78**, 075303 (2008).
[13] Y. Yamauchi *et al.*, Phys. Rev. B **79**, 161306(R) (2009).
[14] C. Altimiras, H. le Sueur, U. Gennser, A. Cavanna, D. Mailly, and F. Pierre, Phys. Rev. Lett. **105**, 226804 (2010).
[15] V. S.-W. Chung, P. Samuelsson, and M. Büttiker, Phys. Rev. B **72**, 125320 (2005).
[16] While we have not measured the temperature dependence of $\mathcal{V}$ when the loops are formed, for higher gate voltages the base temperature visibility has systematically varied like T_φ^{-1}.
[17] G. Seelig and M. Buttiker, Phys. Rev. B **64**, 245313 (2001).
[18] I. P. Levkivskyi and E. V. Sukhorukov, Phys. Rev. B **78**, 045322 (2008).
[19] I. Neder, M. Heiblum, Y. Levinson, D. Mahalu, and V. Umansky, Phys. Rev. Lett. **96**, 016804 (2006).
[20] See Supplemental Material at http://link.aps.org/supplemental/10.1103/PhysRevLett.108.256802 in which we show that thermal averaging is negligible in our experiment. We also discuss in detail the which-path experiment and the fitting procedure allowing us to extract the parameters of the lobe structure V_l and V_C.